05

Mechanical characteristics of marine-grade aluminum alloys at high loading rates

© G.G. Savenkov,^{1,2} T.I. Sycheva,² E.V. Shchukina,² V.Vas. Balandin,³ A.M. Bragov³

¹St. Petersburg State Technological Institute (Technical University),

190013 St. Petersburg, Russia

²Concern Sea Underwater Weapon Gidropribor,

194044 St. Petersburg, Russia

³Lobachevsky State University,

603950 Nizhny Novgorod, Russia

e-mail: sav-georgij@yandex.ru

Received February 4, 2025

Revised March 17, 2025

Accepted April 11, 2025

The results of experimental studies to determine the dynamic characteristics of aluminum alloys 1561 and 1575-1 at strain rates of $\sim 10^3$ and $\sim 10^4 \, \rm s^{-1}$ are presented. Tests at a strain rate of $10^3 \, \rm s^{-1}$ were carried out on an installation implementing the Hopkinson split rod technique. Tests at a strain rate of $10^4 \, \rm s^{-1}$ were carried out on an installation using the method of flat impactor impact with a target (sample) by recording the velocity of the free surface of the sample with an interferometer VISAR. The structure of flat samples after testing is considered. It is established that the relief of the destroyed surface at high impact velocities (> $300 \, \rm m/s$) is formed due to the chaotic fusion of pores and fractures of stratification of various shapes.

Keywords: aluminum alloys, Hopkinson split rod, deflection strength, dynamic strength, microstructure.

DOI: 10.61011/TP.2025.08.61735.16-25

Introduction

Modern frame structures made of new and innovative materials often act in conditions of high-speed (explosive, impact) effect. For this reason, designers and engineers involved in developing and operating such products usually face two problems. Either providing operation of the structure, or arranging a controlled process of fracture. Both the cases require knowledge of characteristics of materials at high strain rates that are inherent in explosive and impact effects. At this, it is desirable to cover the widest possible range of the strain rates, for example, from 10^3 to $10^5\,\mathrm{s^{-1}}$. The lower limit $(10^3\,\mathrm{s^{-1}})$ is typical for low-velocity impacts (below $100\,\mathrm{m/s}$), while the upper limit $(10^5\,\mathrm{s^{-1}})$ is typical for high-velocity impacts $(\sim 1000\,\mathrm{m/s})$ and explosive loads.

Presently, there are several methods of determining the dynamic characteristics, wherein the most common of them are the Kolsky method using the Hopkinson split rod technique (HSR) and the method of high-rate loading of flat targets (tested samples) in conditions of uniaxial strain [1,2].

In the first method one can obtain the mechanical characteristics of a material both in tension and compression. The second method can provide them only in tension, wherein only one mechanical characteristic can be defined, i.e. critical fracture stress: either spallation resistance (when the sample has very few microcracks), or spallation strength (when the sample has a trunk crack or a spallation plate) [3].

The second method is related to spallation fracture of the material in loading and unloading waves, which are a result of reflection of the compression waves from free surfaces [2,4].

By now a large number of structural metals and alloys, including various grades of aluminum and aluminum alloys is included in a quite big database (that is created by results of experiments within the framework of the said method [1–6]) for their dynamic characteristics.

However, there is no investigation of dynamic properties of some corrosion-resistant welded aluminum alloys that are applied in structures of high-speed vessels, dynamically-supported vessels and in some other structures [7]. These alloys include a medium-strength alloy 1561 of the Al–Mg system and a high-strength alloy 1575-1 of the Al–Mg–Sc system. The latter contains 0.12%–0.2% of Sc [7], which, as known [8], ensures a substantial increase of the main strength characteristics, yield strength and ultimate strength as compared to the alloy 1561.

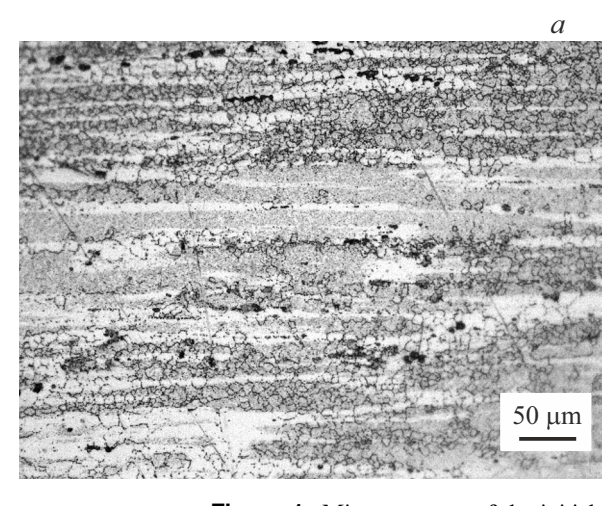
Therefore, based on the above said, the present study is dedicated to investigating high-rate strain and fracture of the said alloys and determining their dynamic characteristics.

1. Materials and techniques of tests

The mechanical characteristics of the studied aluminum alloys 1561 and 1575-1 in tension as per GOST 1497-23 are given in Table 1. The tests were carried out on proportional cylindrical samples of the type III with an initial diameter $d_0 = 5 \, \mathrm{mm}$ and a working length $l_0 = 5 d_0$ in the tester W+b LFM-50.

Material	Ultimate tensile strength σ_b , MPa	Yield strength $\sigma_{0.2}, \mathrm{MPa}$	Relative elongation δ_5 , %	Relative contraction $\psi,\%$
1561 1575-1	345 ± 5 400 ± 5	180 ± 5 270 ± 5	20 ± 1.5 17 ± 1.5	$26 \pm 1 \\ 24 \pm 1$

Table 1. Standard mechanical characteristics of aluminum alloys in tension



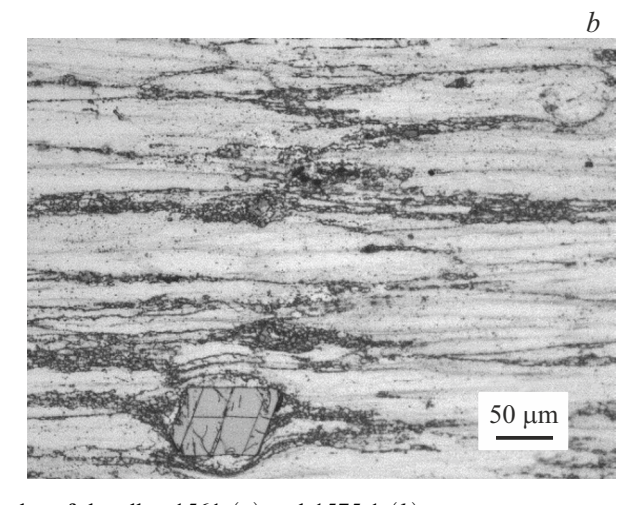


Figure 1. Microstructure of the initial samples of the alloy 1561 (a) and 1575-1 (b).



Figure 2. Tension sample for tests in HSR.

The samples were metallographically studied in the light microscope "Observier.Z.1m". They were etched by a Keller reagent [9]. The microstructure of the initial samples of the alloys is shown in Fig. 1.

The alloy 1561 has a fine-grained structure with insignificant-size inclusions of dispersed phases (Fig. 1, a).

Unlike the alloy 1561 the alloy 1575-1 exhibits a more inhomogeneous structure with large intermetallic compunds of the Al_3Sc scandium phase (Fig. 1, b).

The dynamic characteristics at the strain rates $\dot{\epsilon} \sim 10^3 \, \rm s^{-1}$ were determined by the Kolsky method using the Hopkinson split rod technique [1,10,11] in the installation HSR-20 with the gas gun PG-20, two measuring rods of the diameter of 20 mm and as a set of measurement-recording equipment.

The test samples were shaped as shown in Fig. 2, the diameter of the working part of the sample was 5 mm, the length thereof was 10 mm and the full length of the sample was 40 mm. Three samples were tested per each loading rate, wherein the strain rate was obtained with accuracy $\pm 5\%$ [12].

A dynamic diagram of strain (tension) of the samples within the Hopkinson technique was plotted in the coordinates "true stress" (σ_{tr}) — "true (logarithmic) strain" (ε_{tr}) .

The true stress was calculated by the formula (1), while the logarithmic strain was calculated by the formula (2) [13]:

$$\sigma_{tr} = \sigma(t)(1 + \varepsilon(t)),$$
 (1)

$$\varepsilon_{tr} = \ln(1 + \varepsilon(t)),$$
 (2)

where $\sigma(t)$ — the average stress in the sample at the time strength t, $\varepsilon(t)$ — the average relative strain of the sample at the same time strength t [10].

The spallation strength of the materials was determined in the tester PG-57, which is the gas gun that has a double-diaphragm shutter and is operated by means of compressed air. The installation is designed to obtain the impact velocities from 50 to 500 m/s. The velocity of the free surface is recorded using the interferometer VISAR. A source of radiation for the interferometer is a single-mode and single-frequency neodymium laser Verdy-2 with the radiation wavelength of 0.53 nm. The setup of the installation is shown in Fig. 3.

Strikers were discs of the diameter of 52 mm and the thickness of 3 mm, which were made of an aluminum alloy of the same grade as the tested samples (the discs of the diameter of 92 mm and the thickness of 6 mm).

Obtaining a spallation impulse is assumed to be appearance of the first minimum of the dependence of a spallation surface on time. The obtained dependence is used to

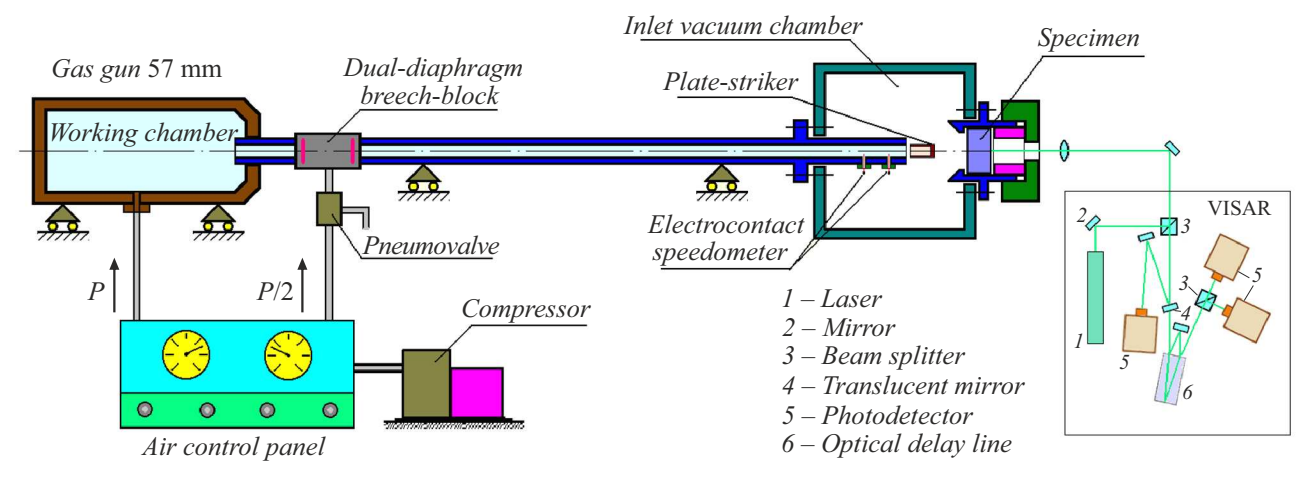


Figure 3. Setup of the installation PG-57 for determining spallation strength.

determine the following characteristics: the maximum W_1 and the minimum W_2 velocity of the free surface, the time of velocity drop from the maximum to the minimum.

The maximum tensile stresses σ_p and the strain rate $\dot{\varepsilon}$ are calculated by the formulas (3) and (4):

$$\sigma_p = 0.5 \rho_0 c_0 (W_1 - W_2), \tag{3}$$

$$\dot{\varepsilon} = \frac{1}{c_0} \frac{\partial W_1}{\partial t},\tag{4}$$

where ρ_0 — the density of the sample material (it is $2650 \, \text{kg/m}^3$ for the studied materials), the volume speed of sound (5240 m/s). As noted above, when there is the trunk crack inside the sample (spallation), which is found when cutting the sample, the maximum tensile stresses σ_p correspond to the spallation strength, but otherwise (very few cracks) they characterize the spallation resistance [3]. Generally, σ_p is a characteristic of the material strength at the strain rates $10^4 - 10^5 \, \text{s}^{-1}$.

2. Results of mechanical tests and their analysis

2.1. Dynamic tension tests in HSR

Results of tests of the samples made of the aluminum alloys 1561 and 1575-1 in HSR are shown in Table 2 (it specifies true values of dynamic ultimate strength and yield strength). Typical diagrams of dynamic strain of the samples are shown in Fig. 4.

Results for impact tension (Table 2) have been compares with results of the standard tests (Table 1) to show that within the rate range $(1.5-3)\cdot 10^3\,\mathrm{s^{-1}}$ for the alloy 1561 the yield strength sharply increases (by $25\,\%-80\,\%$) and in a lesser extent the ultimate strength sharply increases (by $25\,\%-33\,\%$) at the strain rates $(2.5-3.0)\cdot 10^3\,\mathrm{s^{-1}}$). There is also increase of the yield strength and the ultimate strength for the alloy 1575-1 (although in a lesser extent than for the alloy 1561). At the same time, the plasticity

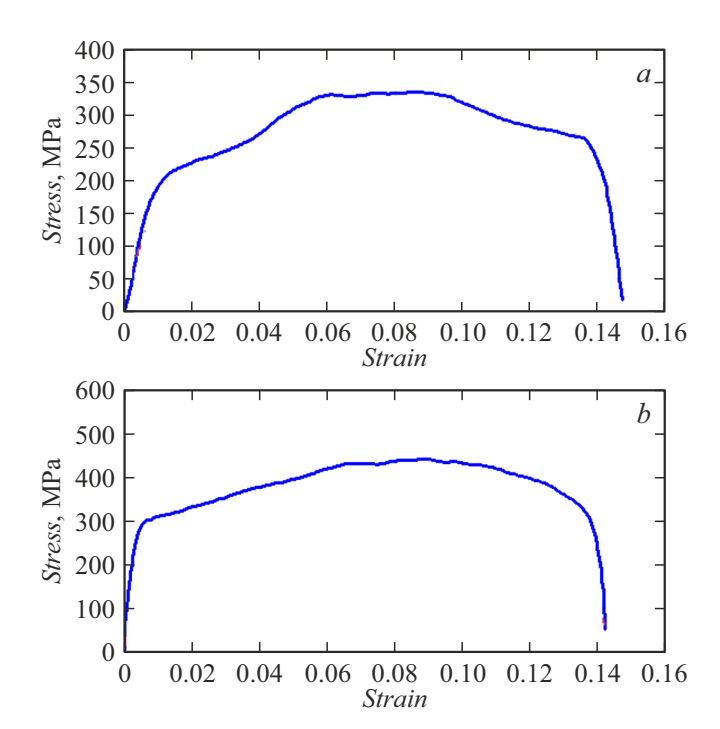


Figure 4. Diagrams of strain of the alloy 1561 (a) and the alloy 1575-1 (b) at the strain rate of 1500 s⁻¹.

characteristic of the alloys (the relative contraction ψ) remained almost unchanged. It is incorrect to compare by the relative elongation due to a different length of the samples l_0 and the working diameter d_0 (and, as a consequence, a different ratio l_0/d_0 [13]) for the static and dynamic tests.

2.2. Tests for determining spallation characteristics

The results of tests of the samples made of the aluminum alloys in the installation PG-57 are shown in Fig. 3, while

Alloy grade	Strain rate $\dot{\varepsilon}$, s ⁻¹	Dynamic yield strength σ_{sd} , MPa	Dynamic ultimate strength σ_{bd} , MPa	Relative elongation δ_d , %	Relative contraction $\psi_d, \%$
1561	1500 ± 10 2500 ± 10 3000 ± 10	225 ± 15 300 ± 10 325 ± 10	345 ± 5 430 ± 15 460 ± 15	16 ± 1 19 ± 1 20 ± 1	24 ± 1 26 ± 1.5 26 ± 2
1575-1	1500 ± 10 2000 ± 10 3000 ± 10	310 ± 30 340 ± 10 385 ± 15	450 ± 5 475 ± 5 540 ± 10	$ \begin{array}{c} 14 \pm 1 \\ 13 \pm 0.5 \\ 10 \pm 0.5 \end{array} $	23 ± 1 21 ± 1 19 ± 1

Table 2. Dynamic properties of the aluminum alloys in tension

Table 3. Results of dynamic strength tests of the alloys

Material of the sample	Impact velocity, m/s	Strain rate, s ⁻¹	Spallation strength, MPa
Alloy 1561	$ \begin{array}{c} 150 \pm 20 \\ 250 \pm 20 \\ 350 \pm 20 \\ 420 \end{array} $	$8.3 \cdot 10^{3}$ $10.6 \cdot 10^{3}$ $15.7 \cdot 10^{3}$ $16.2 \cdot 10^{3}$	470 ± 10 470 ± 10 480 ± 15 540 ± 5
Alloy 1575-1	150 ± 25 250 ± 10 350 ± 15	$8.3 \cdot 10^{3}$ $10.2 \cdot 10^{3}$ $11.6 \cdot 10^{3}$	400 ± 20 410 ± 15 570 ± 15

the typical curves of the velocity of the free surface of the samples are shown in Fig. 5.

The results obtained for the dynamic characteristics shown in Tables 2 and 3 have been analyzed to show that values of the true ultimate strengths, which were obtained in the HSR tests at the strain rates $(1.5-3)\cdot 10^3\,\mathrm{s^{-1}}$ for the both the alloys, are almost identical to values of the spallation strength at the strain rates $(8.3-16.2)\cdot 10^3\,\mathrm{s^{-1}}$. This result well complies with results of the study [14], which has shown by examples of steels of various grades, copper and a titanium alloy that at the strain rate $5\cdot 10^3\,\mathrm{s^{-1}}$ values of true rupture resistance are almost identical to the values of spallation strength.

It follows from the presented results that starting with a certain strain rate there is a growth of the characteristics of dynamic strength (spallation strength).

2.3. Results of metallographic analysis

Only the flat samples were metallographically analyzed and results of microstructure studies of the fractured samples after being tested in HSR will be given in a separate article.

Since the microstructure studies of the samples made of aluminum and the aluminum alloys after spallation fracture have been performed in many papers [6,15–18] et al.], in our case the samples were metallographically analyzed, first of all, in order to identify certain specific features of the process of spallation fracture only, which had not been

observed previously in these alloys. For this purpose, the tested samples were cut along an impact direction by the diameter and the microstructure was studied on a produced surface. We note the following fact. Table 3 shows results of determination of the spallation strength except for the results for both the alloys at the impact velocities $(150\pm25)\,\text{m/s}$. No trunk crack was observed in these samples, i.e. respective lines contain characteristics of the spallation resistance.

2.4. Results of metallographic analysis of the samples made of the alloy 1561

The structure of the samples made of the alloy 1561 subsequently exhibits: at the impact velocities $\sim 150\,\mathrm{m/s}$ — delamination cracks in bedding locations of dispersed phases and small dynamically recrystallized grains (Fig. 6, a), while with increase of the impact velocity ($\sim 170 \, \text{m/s}$) the delamination cracks enlarge, including by formation of micropores and their merging (Fig. 6, b). The delamination cracks are directed along propagation of a shock wave and their formation seems to be related to velocity inhomogeneity of a medium [6,19]. With the impact velocities $> 210 \,\mathrm{m/s}$ the pores enlarge and merge to form break-off cracks and the trunk crack is formed, while very few locations exhibit localization of strain by the adiabatic section (Fig. 6, c). The break-off cracks are directed perpendicular to a direction of propagation of the shock wave. Finally, with the impact velocities of $\sim 300 \, \text{m/s}$ and higher a spallation "plate" is

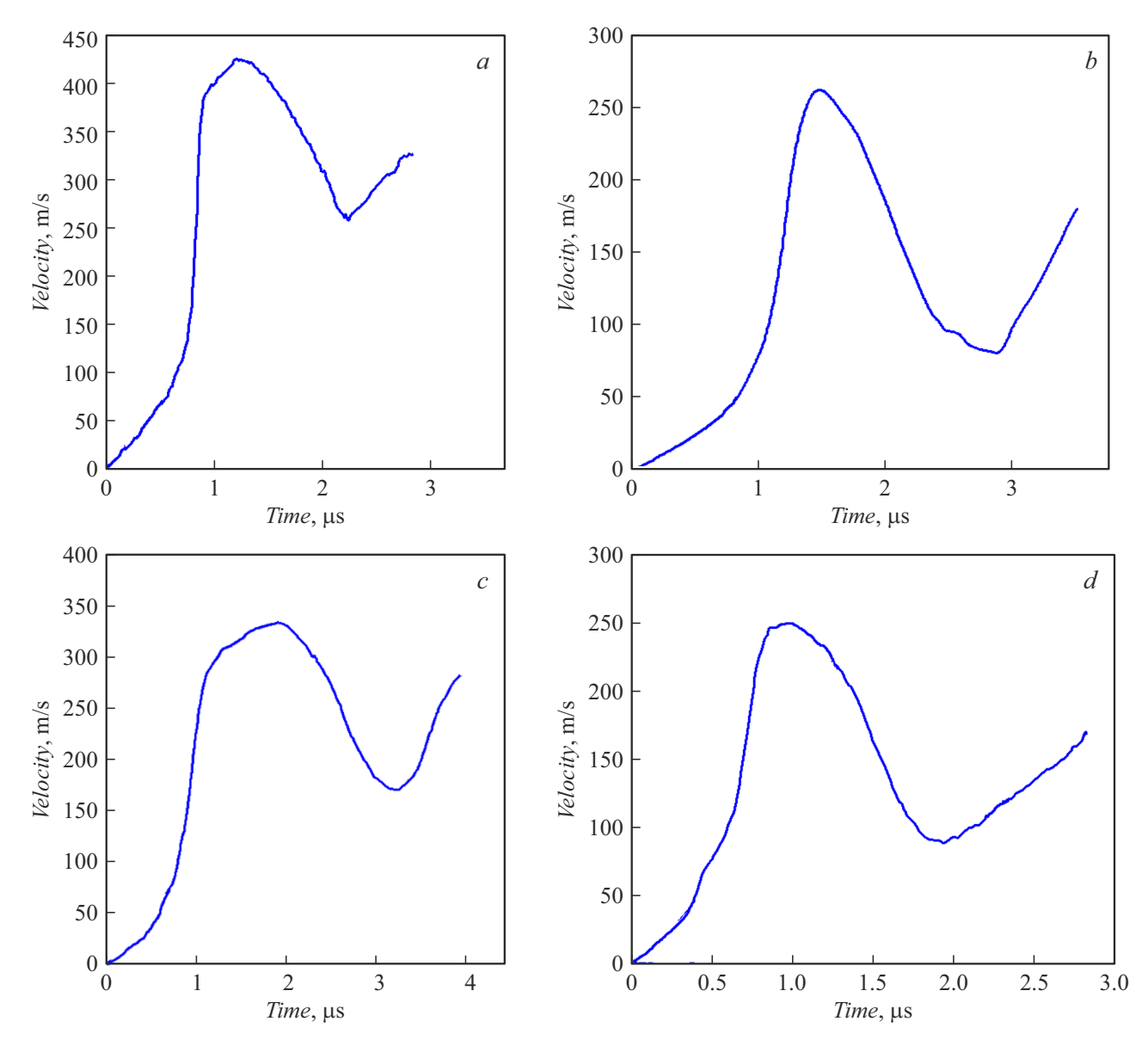


Figure 5. Typical oscillograms of the velocity of the free surface for the aluminum alloys 1561 (a, b) and 1575-1 (c, d) at the impact velocities 420, 270, 340, 250 m/s, respectively.

formed, while a relief of the remaining part of the sample is a surface that is formed by chaotic merging of pores and the delamination cracks that have a various form (Fig. 6, d). Chaotization of pore merging is probably caused by instability of plastic strain due to a difference of its rates in adjacent areas of plastic flow. In turn, a difference of the strain rates in the adjacent areas is due to dispersion of the material particle velocities [6,19].

2.5. Results of metallographic analysis of the samples made of the alloy 1575-1

In the structure of the samples made of the alloy 1575-1 after the tests at the impact velocities \sim 140 m/s a dynamic effect is manifested in increase of a number of brittle

cracks in the intermetallic compounds and their enlargement (Fig. 7, a), while the delamination cracks are practically absent. It can be assumed that the intermetallic inclusions serve as effective foci of dissipation of the shock wave. The delamination cracks begin to appear, so do the micropores, at the impact velocities of ~ 175 m/s. Then, at the velocities > 220 m/s, as in the case of the alloy 1561, the micropores enlarge and merge to form the break-off cracks and the trunk crack is formed (Fig. 7, c). With the impact velocities of ~ 300 m/s and higher, as in the case of the alloy 1561, a spallation "plate" is formed while a relief of the remaining part of the sample is a surface that is formed by merging of the pores and the delamination cracks that have a various form (Fig. 7, d, e). At the same time, a relief structure is more ordered than in the alloy 1561, which may indicate

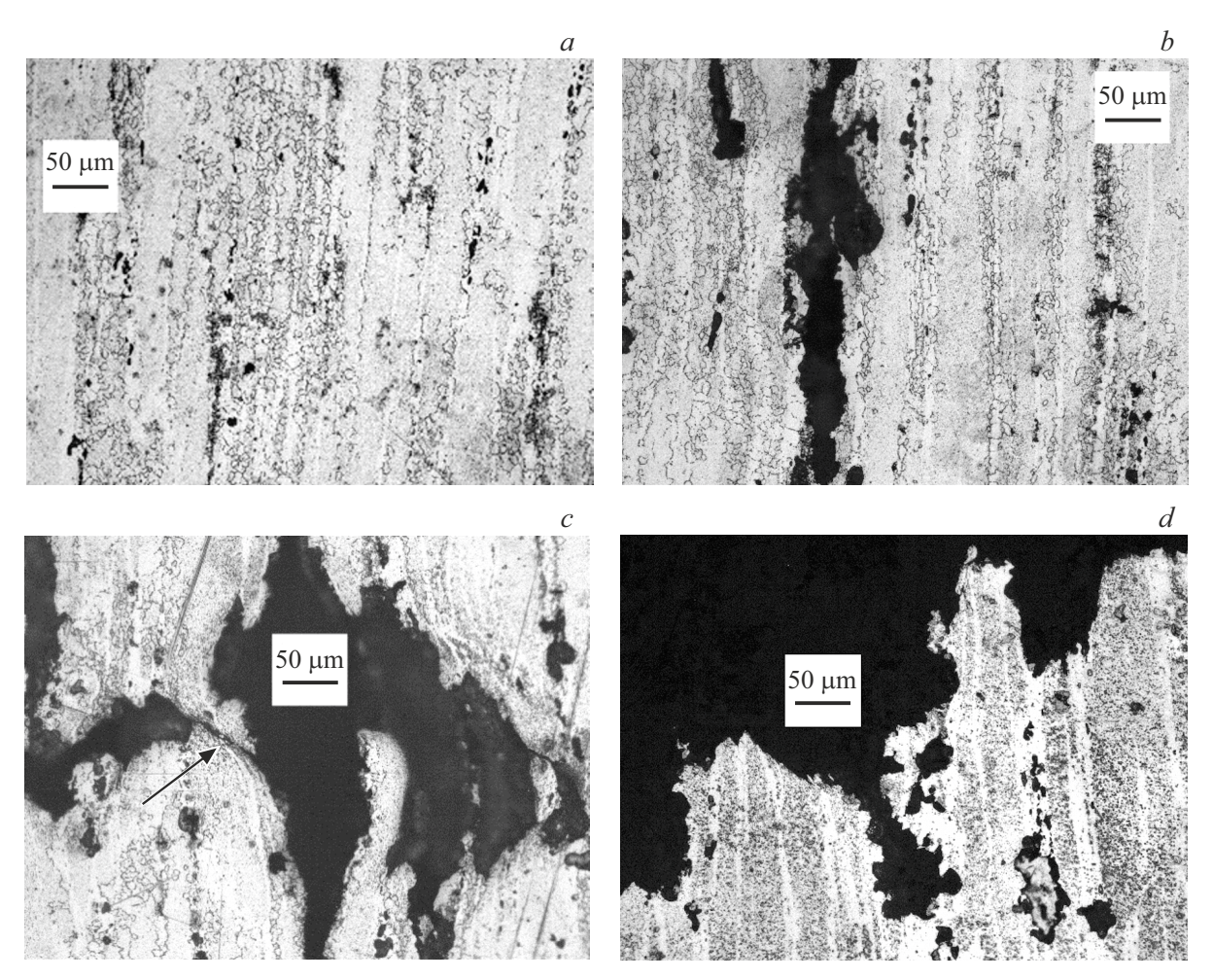


Figure 6. Microstructure of the samples made of the alloy 1561 after impact. The fragments a-d show the impact velocity of 150, 170, 270 and 320 m/s, respectively. The arrow indicates an adiabatic section.

lesser dispersion of the medium particle velocities under dynamic loading.

It should be noted that in our case contours of the trunk crack and a fracture surface differ from similar forms in the samples made of the alloy 1565 [20] that belongs to the same group of the aluminum alloys [7] as those investigated in the present study. In the alloy 1565 the contour of the trunk crack and, respectively, the contour of the fracture surface have a pronounced step-wise form.

Conclusion

The performed experimental studies suggest the following conclusions:

- 1) the aluminum alloys 1561 and 1575-1 have the high specific dynamic strength, so they can be recommended as structural materials for products that must have a relatively small weight and operate in conditions of extreme external loads:
- 2) with lesser values of the static strength, the alloy 1561 is more susceptible than the alloy 1575-1 to the strain rate

- $\sim 10^3 \, {\rm s}^{-1}$ (its values of the dynamic yield strength and ultimate strength substantially increase in relation to the static values, wherein a plasticity index ψ_d is still the same);
- 3) in comparison with the alloy 1561, with increase of the strain rate to $\sim 10^3 \, \text{s}^{-1}$ the alloy 1575-1 is prone to embrittlement (with increase of the strain rate the plasticity index ψ_d is reduced);
- 4) the values of the true ultimate strengths, which were obtained in the HSR tests at the strain rates $(1.5-3)\cdot 10^3\,s^{-1}$ for the alloys 1561 and 1575-1, are almost identical to values of the spallation strength at the strain rates $(8.3-16.2)\cdot 10^3\,s^{-1}.$

Funding

This study was financially supported by the Ministry of Education and Science of the Russian Federation under State assignment (project N_2 FSWR-2023-0036).

Conflict of interest

The authors declare that they have no conflict of interest.

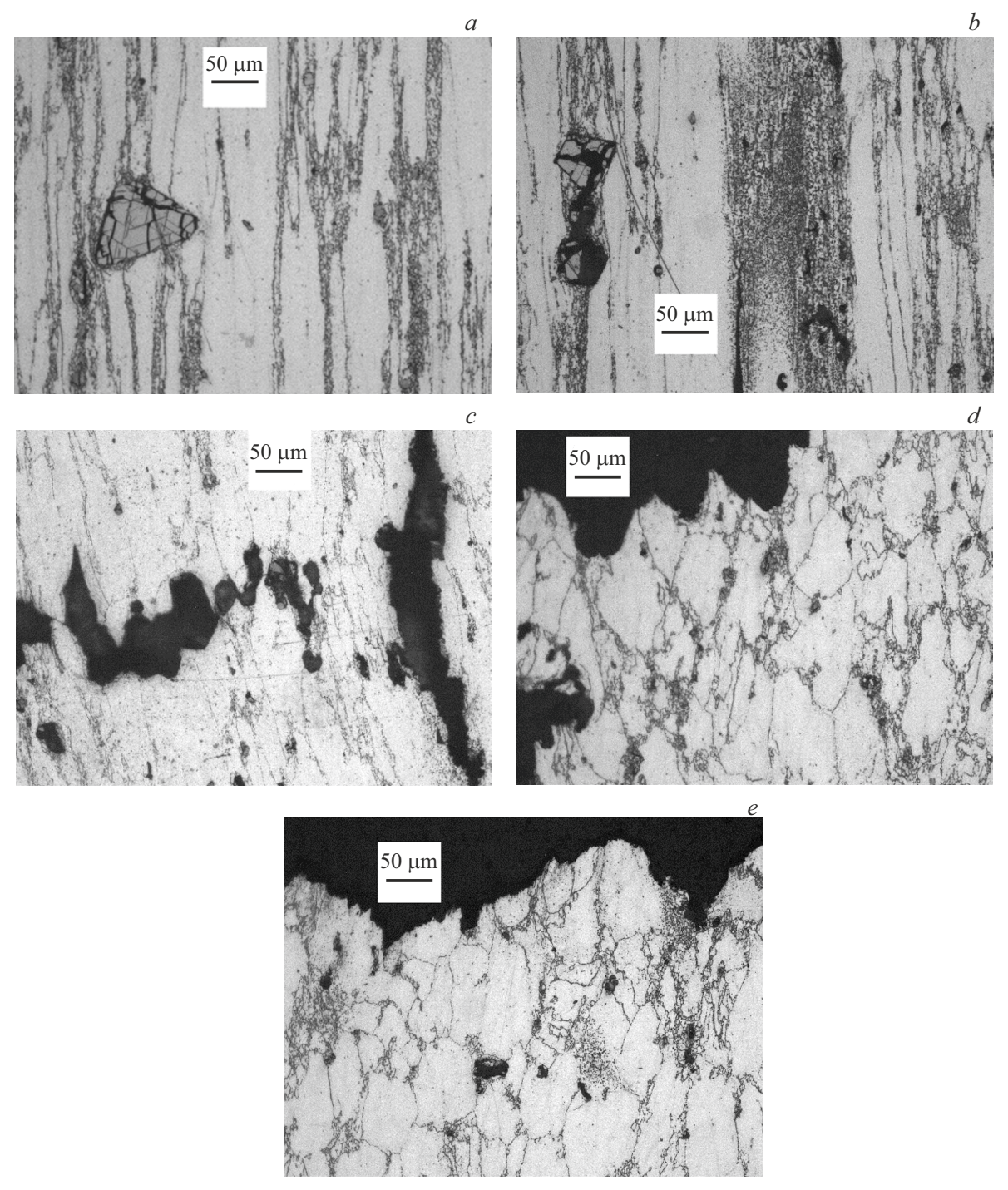


Figure 7. Microstructure of the samples made of the alloy 1575-1 after impact. The fragments a-d, e show the impact velocity of 137, 176, 250, 340 m/s, respectively.

References

- [1] A.M. Bragov, A.K. Lomunov. Ispol'zovanie metoda Kol'skogo dlya issledovaniya protsessov vysokoskorostnogo deformirovaniya materialov razlichnoi fizicheskoi prirody (Izdvo Nizhegorodskogo gos. un-ta, Nizhnii Novgorod, 2017), 148 s. (in Russian).
- [2] Razrushenie raznomasshtabnykh ob'ektov pri vzryve, pod obshch red. A.G. Ivanova (RFYaTs.VNIIEF, Sarov, 2001), 482 s. (in Russian).
- [3] G.G. Savenkov, A.V. Kuznetsov, A.M. Bragov. ZhTF, **88** (5), 740 (2018) (in Russian).
- [4] B.L. Glushak, I.R. Trunin, S.A. Novikov, A.I. Ruzanov. *Fraktaly v prikladnoi fizike*, pod obshchei red. A.E. Dubinova (Arzamas-16, 1995), s. 59–122 (in Russian).

- [5] G.I. Kanel', S.V. Razorenov, A.V. Utkin, V.E. Fortov. *Udarno-volnovye yavleniya v kondensirovannykh sredakh* (Yanus-K, M., 1996), 408 s. (in Russian).
- [6] Yu.I. Meschcheryakov. Mnogomasshtabnye udarno-volnovye protsessy v tverdykh telakh (Nestor-Istoriya, SPb., 2018), 480 s. (in Russian).
- [7] E.P. Osokin, N.N. Barakhtina, V.I. Pavlova, E.A. Alifirenko, S.A. Zykov. Tekhnologiya legkikh splavov, 3, 69 (2022) (in Russian). DOI: 10.24412/0321-4664-2022-3-69-84
- [8] V.V. Zakharov, A.I. Fesenko. Tekhnologiya legkikh splavov, 4, 40 (2015) (in Russian).
- [9] A.I. Baluev, L.A. Bozina, G.I. Nikolaev, V.V. Obukhovskii, K.I. Khvostyntsev. *Prakticheskoe rukovodstvo po metallo-grafii sudostroitel'nykh materialov* (Izd-vo Sudostroenie, L., 1982), 136 s. 48 s. (in Russian).
- [10] A.M. Bragov, L.A. Igumnov, A.Yu. Konstantinov, A.K. Lomunov. *Vysokoskorostnaya deformatsiya materialov* (Izd-vo Nizhegorodskogo gos. un-ta, Nizhnii Novgorod, 2020), 300 s. (in Russian).
- [11] A.M. Kuz'min, A.Yu. Konstantinov, G.G. Savenkov. ZhTF, 94 (10), 1688 (2024) (in Russian). DOI: 10.61011/JTF.2024.10.58862.201-24
- [12] A.M. Bragov, A.V. Kuznetsov, G.G. Savenkov, T.I. Sycheva, E.V. Shchukina. PMTF, 62 (1), 119 (2021) (in Russian).
- [13] N.A. Shaposhnikov. *Mekhanicheskie ispytaniya metallov* (Mashgiz, M.-L., 1951), 384 s. (in Russian).
- [14] G.G. Savenkov. PMTF, 46 (6), 103 (2005) (in Russian).
- [15] A.K. Divakov, L.S. Kokhanchik, Yu.I. Meshcheryakov, M.M. Myshlyaev. PMTF, 3, 135 (1987) (in Russian).
- [16] I.G. Brodova, A.N. Petrova, S.V. Razorenov, E.V. Sholokhov. Fizika metallov i metallovedenie, 116 (5), 548 (2015) (in Russian).
- [17] Yu.V. Petrov, S.A. Atroshenko, N.A. Kazarionov, A.D. Evstifeev, V.Yu. Solov'ev. FTT, **59** (4), 648 (2017) (in Russian).
- [18] I.N. Borodin, A.E. Maier, S.A. Atroshenko. Bazovyi masshtabnyi uroven' otkol'nogo razrusheniya v chistom alyuminii i ego splave D16: mikorstrukturnye issledovaniya i chislennoe modelirovanie// Fiziko-khimicheskie aspekty predel'nykh sostoyanii i strukturnykh prevrashchenii v sploshnykh sredakh, materialakh i tekhnicheskikh systemakh, 1, 208 (2017) (in Russian).
- [19] Yu.I. Meshcherykov, A.K. Divakov. Interferentsionnyi metod registratsii skorostnoi neodnorodnosti chastits v uprugoplasticheskikh volnakh nagruzki v tverdykh telakh (LFI-Mash, L., 1989), 36 s. (in Russian).
- [20] A.K. Divakov, N.I. Zhigacheva, G.V. Konovalov, Yu.I. Meshcheryakov, E.P. Osokin. Pis'ma v ZhTF, **45** (5), 34 (2019) (in Russian).

Translated by M.Shevelev